

● Development of oxide-based ceramic matrix composites with high thermal stability

Advanced Materials Research Laboratory, TOSOH Corporation

Yushi NAWATA
Ikuya OHTA
Yo HIRATAKA
Isao YAMASHITA

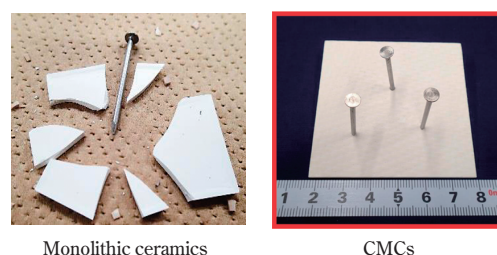
1. Introduction

Ceramic matrix composites (CMCs) exhibit an interesting combination of low density, damage tolerance, and high-temperature mechanical properties. Thus, these materials have potential application in thermal resistance materials, aircraft engines, and power generation turbines as conventional nickel super alloys.¹⁻³ For aircraft gas turbine engines, the efficiency improvement obtained using CMCs is $\sim 6.5\%$ due to fuel efficiency improvements, and approximately 100 million tons of CO₂ reduction is expected by 2035 due to the use of CMCs⁴. **Figure 1** shows monolithic ceramics and CMCs after performing a nail penetration test. The monolithic ceramics exhibit fully brittle failure; however, the CMCs maintain their shape due to their high damage tolerance. **Figure 2** shows the damage tolerance mechanism of the CMCs. Three microstructural concepts are considered for enabling crack deflection at fiber-matrix interface⁵. High damage

tolerance of CMCs is achieved by crack deflection along the weak fiber-matrix interface, uncollected fiber failure and energy dissipation during fiber pullout.

Oxide-based CMCs (Ox/Ox) composed of oxide fibers and an oxide matrix involve a simpler preparation process, have a lower cost, and exhibit good corrosion resistance compared to SiC-based CMCs⁶. Thus, Ox/Ox are promising for high-temperature applications in various oxidizing environments⁷.

However, the primary limitation of Ox/Ox in practical applications is their thermal stability. Previous



Monolithic ceramics

CMCs

Fig. 1 Nail penetration test

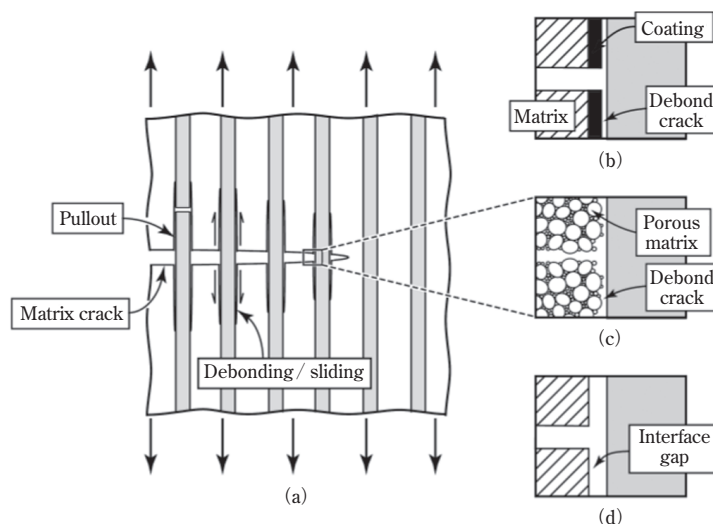


Fig. 2 Damage tolerance mechanism of CMCs⁵

commercially available Ox/Ox degrade after long-term thermal exposure at up to 1200 °C. The bending stresses of UMOX™ (EADS Innovation Works), WHIPOX™ (DLR), and OXIPOL (DLR) are reduced by approximately 20%–50% after thermal exposure at 1200 °C temperatures for 50 h⁸. Additionally, the tensile strength of Ox/Ox (Composite Horizons, 3M Company, and Axiom Materials, Inc.) are reduced by ~ 25% after being exposed to a temperature of 1200 °C for 500 h⁹. The tensile strength of N610/AS and N720/AS (ATK-COIC) is reduced by approximately 68%–79% after exposure at 1200 °C for 100 h¹⁰ and that of N720/A (ATK-COIC) is reduced by 12% after exposure at 1200 °C for 1000 h^{11,12}. The tensile strength of Nextel610 / monazite/alumina composite (Air Force Research Laboratory) is reduced by 38% after exposure at 1200 °C for 1000 h¹³. The degradation of Ox/Ox after thermal exposure is due to the enhancement of the fiber–matrix interface bonding and, most importantly, thermal degradation of the reinforcing fibers. Fiber degradation due to grain growth is the most essential problem for oxide fibers. The size of crack inducing flaws correlate well to the grain size of oxide fibers. Fiber strength of Nextel 610, Nextel650, Nextel720 (3M Company) is clearly affected by grain size¹⁴.

Thus, we have developed the uniform doping method (UDM) to suppress the grain growth of oxide fibers and novel Ox/Ox that exhibit high thermal stability. In this report, the proposed UDM for oxide fibers and the mechanical properties of the developed Ox/Ox are summarized. The purpose of our development is to achieve Sustainable Development Goal 7 (Affordable and Clean Energy) and contribute to society by providing novel Ox/Ox.

2. Proposed UDM for oxide fibers

The proposed UDM is based on the uniform doping of a grain growth inhibitor element into ceramics fiber (Figure 3). During thermal exposure, grain growth occurs, which reduces strength, and the fibers treated by the proposed UDM exhibit suppressed grain growth and retained strength. Figure 4 shows a high-resolution transmission electron microscopy with energy-dispersive spectroscopy (TEM-EDS) mapping of the

doping element in mullite fibers. The doped element is distributed uniformly and segregated in the grain boundary.

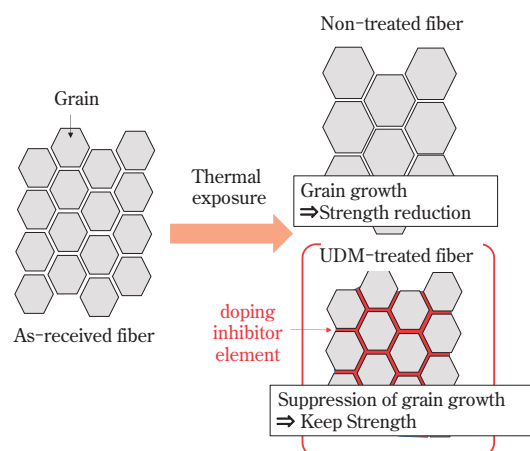


Fig. 3 Concept of uniform doping methods (UDM)

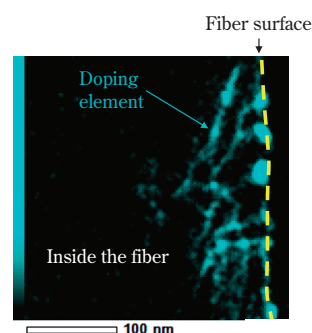


Fig. 4 High resolution TEM-EDS mapping of doping element in mullite fiber

Figure 5 shows the relative single-filament tensile strength of fibers treated using the proposed UDM compared to untreated fibers. The tensile strength of fibers was evaluated following JIS R1657. Here, we applied UDM treatment to alumina fiber and mullite fiber. The tensile strength of the alumina and mullite fibers was improved after thermal exposure at 1300 °C for 100 h with the proposed UDM. Figure 6 shows a scanning electron microscope (SEM) image of the surface of UDM-treated alumina fiber after thermal exposure at 1300 °C for 100 h and a SEM image of the untreated fiber. Many abnormal grain growths are observed in the untreated fiber, whereas the suppression of grain growth can be observed in the fiber treated by the proposed UDM.

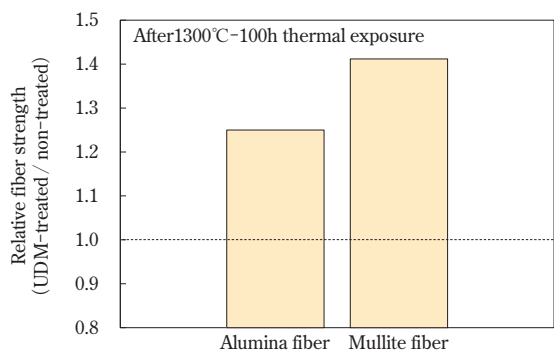


Fig. 5 Relative fiber strength after thermal exposure at 1300°C for 100h

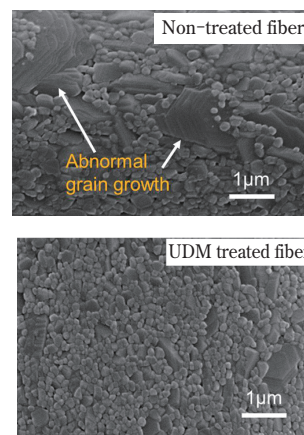


Fig. 6 Surface appearance of alumina fiber after thermal exposure at 1300°C for 100h

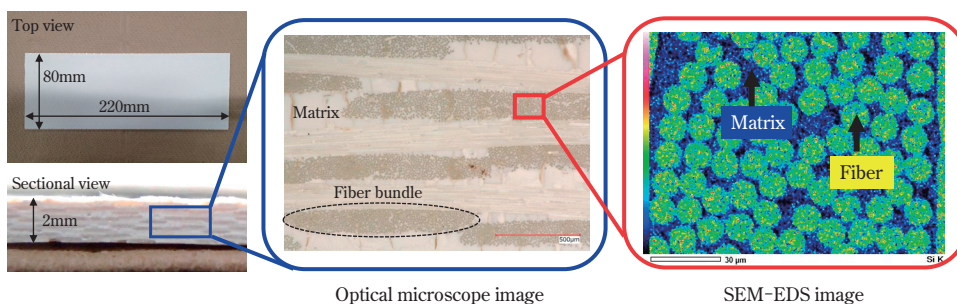


Fig. 7 Optical image and microstructure of Ox/Ox using UDM-treated fiber

3. Appearance and microstructure of Ox/Ox using UDM-treated fibers

Ox/Ox were developed using UDM-treated fibers and an alumina-based matrix fabricated by slurry infiltration and sintering process. Figure 7 shows optical and SEM-EDS images of a fabricated plate type of Ox/Ox. The plate of five woven layers Ox/Ox had 220 by 80 mm rectangular shape with a thickness of 2 mm. Additionally, matrix phase filled between the piled woven layers and inside the fiber bundles. The developed CMCs can be fabricated into various shapes, e.g., a cylindrical shape (Figure 8), using slurry infiltration and sintering process.

4. Mechanical properties of Ox/Ox at room temperature

The mechanical properties at room temperature of the developed Ox/Ox are given in Table 1. Figure 9 shows stress-strain curves and shape and dimension

of the test specimen. Here, TCA-01 is an alumina fiber-based CMC, and TCM-01 is mullite fiber-based CMC using UDM-treated fibers. In this study, density of the composite was measured following the Archimedes method, and the tensile modulus, tensile strength, and proportional limit (0.05% offset) were evaluated following the American Society for Testing and Materials (ASTM) C1275 standard. Tensile tests were carried out using a

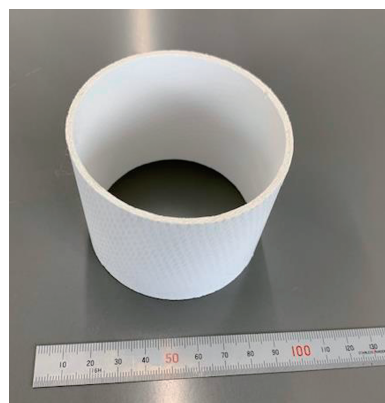


Fig. 8 Cylindrical shape of Ox/Ox

Table 1 Mechanical properties of Ox/Ox using UDM treated fiber at room temperature

CMC	Density [g/cm ³]	Young's modulus ¹⁾ [GPa]	Proportional limit ^{1) 2)} [MPa]	Tensile strength ¹⁾ [MPa]
TCA-01 (Alumina fiber-based)	2.75	73	290	295
TCM-01 (Mullite fiber-based)	2.62	64	140	183

1) Following ASTM C1275, 2) 0.05% Offset Method,

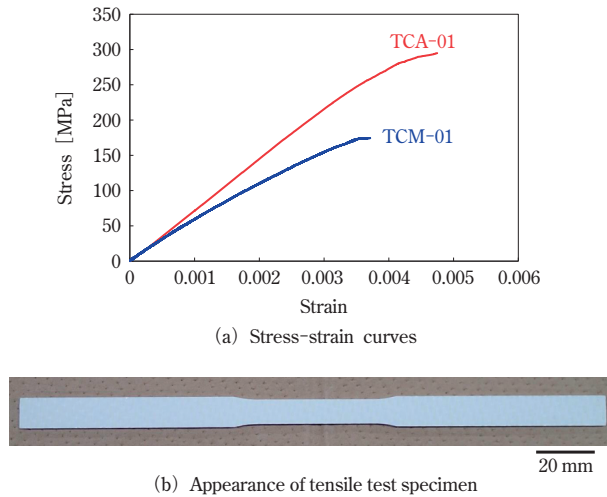


Fig. 9 (a) Stress-strain curves of Ox/Ox and (b) appearance of tensile test specimen

screw-driven type universal mechanical test machine (MTS Criterion™ Model 45 MTS Systems Corporation) and a strain gauge (Model 632.13F-20 MTS Systems Corporation). Here, the constant displacement rate was 0.50 mm/min. Dog bone shaped specimens (200-mm total length with an 8-mm wide gauge section and a thickness of 2 mm) were used. In TCA-01, Young's modulus is >70 GPa, and the tensile strength and proportional limit is >250 MPa. In TCM-01, Young's modulus is >60 GPa, the tensile strength is >150 MPa, and the proportional limit is >100 MPa. Furthermore, thermal conductivity of the developed Ox/Ox was calculated from thermal diffusivity evaluated following ASTM E1461, specific heat, and density. The developed

Ox/Ox exhibited low thermal conductivity (5.6 W/(m·K) for TCA-01, 3.3 W/(m·K) for TCM-01) .

5. Mechanical properties of Ox/Ox at high temperature

High-temperature (1200 °C) tensile tests were conducted based on the ASTM C1359 standard in air using mechanical test machine (MTS808 MTS Systems Corporation) and a strain gauge (MTS632.59F-71 MTS System Corporation). The constant displacement rate was 3.00 mm/min. The mechanical properties of the Ox/Ox at 1200 °C are listed in **Table 2**. **Figure 10** shows stress–strain curves of TCA-01 and TCM-01. The

Table 2 Mechanical properties of Ox/Ox using UDM-treated fibers at 1200°C

CMC	Young's modulus ¹⁾ [GPa]	Proportional limit ^{1) 2)} [MPa]	Tensile strength ¹⁾ [MPa]
TCA-01 (Alumina fiber-based)	83	92	188
TCM-01 (Mullite fiber-based)	56	130	177

1) Following ASTM C1359, 2) 0.05% offset method,

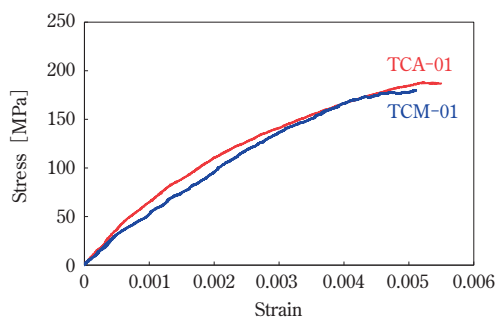


Fig.10 Stress-strain curves of Ox/Ox at 1200°C

shape of the test specimen was the same as that used in the room temperature test. The tensile strength and proportional limit of TCA-01 is degraded compared to the results obtained in the room temperature test. The tensile strength of TCM-01 at 1200 °C was almost same as that that of TCM-01 at room temperature.

6. Thermal exposure test of Ox/Ox

A thermal exposure test was also performed using dog bone shaped specimens 200 mm total length with an 8 mm wide gauge section and a thickness of 2 mm at 1200 °C for 1000 h in air. Here, the temperature during thermal exposure was controlled precisely using an R type thermocouple. **Figure 11** shows the tensile strength of developed Ox/Ox as processed and after thermal exposure at 1200 °C for 1000 h. No remarkable reduction in tensile strength was observed for both TCA-01 and TCM-01 after 1200 °C for 1000 h. Retention rates of TCA-01 and TCM-01 are 96% and 103%. **Figure 12** shows the fracture surface of the tensile test specimens after thermal exposure at 1200 °C for 1000 h.

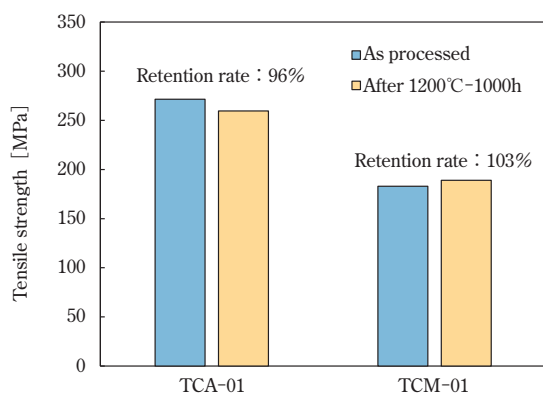


Fig.11 Tensile strength of developed Ox/Ox as processed and after 1200°C for 1000h thermal exposure

The fracture surface clearly exhibits uncorrelated fiber failure and bundle unite fiber pull-out. Thus, both of the developed oxide-based CMCs exhibit damage tolerance after thermal exposure at 1200 °C for 1000 h. **Figure 13** shows tensile strength as processed and retention rate of tensile strength after thermal exposure of TCM-01 and previous commercially available Ox/Ox using mullite fiber. TCM-01 shows higher retention rate of tensile strength than that of others, and high tensile strength as processed.

7. Notch sensitivity test of Ox/Ox

A notch sensitivity test of the Ox/Ox after thermal exposure at 1200 °C for 1000 h was also conducted using tensile specimens containing double-edge notches, as shown in **Figure 14(a)**. **Figure 14(b)** shows the relative tensile strength of the notched and unnotched Ox/Ox at different $2a/W$ (a : notch length and W : specimen width) and the theoretical curve of the relative strength of monolithic ceramics. Note that the strength of monolithic ceramics depends on the size of the defects ($\sigma = \frac{K_I}{\sqrt{\pi a}} f\left(\frac{a}{w}\right)$, K_I is stress intensity factor, $f\left(\frac{a}{w}\right)$ is shape function)¹⁵; thus, the relative strength of monolithic ceramics decreases rapidly as $2a/W$ increases. Here, no remarkable reduction in the relative tensile strength of the developed Ox/Ox was observed with $2a/W$. Thus, these results confirm that the developed Ox/Ox exhibit damage tolerance after thermal exposure at 1200 °C for 1000 h.

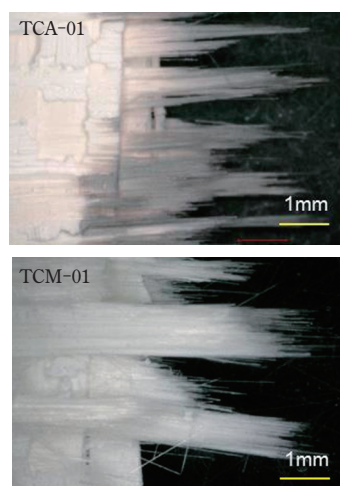


Fig.12 Fracture surface of tensile test specimen after 1200°C-1000h

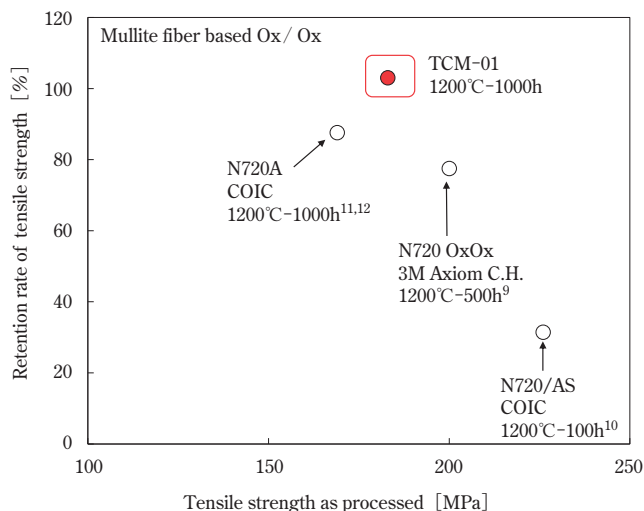


Fig.13 Tensile strength as processed and retention rate of tensile strength after thermal exposure of TCM-01 and previous commercially available Ox/Ox using mullite fiber

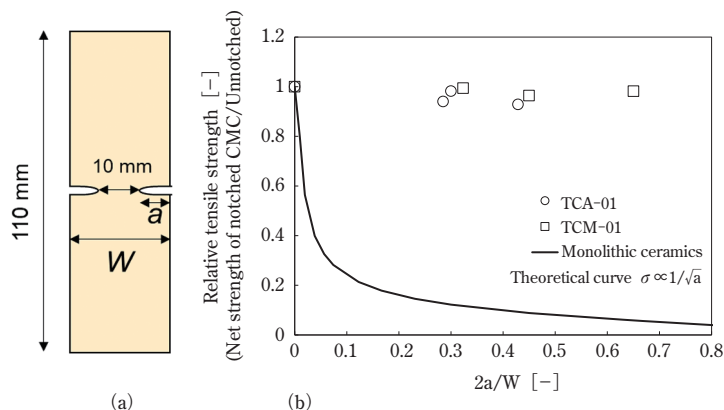


Fig.14 (a) Schematic of test specimen
(b) Notch sensitivity of Ox/Ox after thermal exposure at 1200°C-1000h and theoretical curve of monolithic ceramics,

8. Conclusion

In this report, we have described a method to improve the thermal stability of oxide fibers and the development of two oxide-based CMCs that exhibit high thermal stability. We found that TCA-01 demonstrated high tensile strength and proportional limit (>250 MPa) at room temperature, and TCM-01 maintained a high tensile strength and proportional limit even at 1200 °C. Additionally, the developed CMCs did not demonstrate a reduction in tensile strength after thermal exposure at 1200 °C for 1000 h. The developed Ox/Ox also exhibited low thermal conductivity (5.6 W/(m·K) for TCA-01, 3.3 W/(m·K) for TCM-01). Thus, we consider that the

developed Ox/Ox can be employed in energy related materials, particularly thermal resistance materials, aircraft turbines, and power turbines, where long-term thermal stability and high mechanical properties are required.

Acknowledgments

The authors thank Professors Yutaka Kagawa and Yoshihisa Tanaka at The Center for Ceramics Matrix Composites at Tokyo University of Technology for the use of their evaluation equipment and useful discussions.

References

- 1) T. E. Steyer, *International Journal of Applied Ceramic Technology*, **10**(3),389-394 (2013)
- 2) W. Krenkel et al., *Ceramic Matrix Composites, Fiber Reinforced Ceramics and Their Applications*, 327-349(2014)
- 3) K. A. Keller et al., *Ceramic Matrix Composite: Materials, Modeling and Technology*, 236-272 (2014)
- 4) Business and Project Summary of NEDO, “Reliability Assessment Methodology for Advanced Ceramic Matrix Composites (CMCs)” <https://www.nedo.go.jp/activities/ZZJP_100173.html>
- 5) F. W. Zok, *Journal of the American Ceramic Society*, **89**(11), 3309–3324 (2009)
- 6) K. Ramachandran et al., *Journal of the European Ceramic Society*, **42**(4), 1626–1634 (2022)
- 7) K. Tushtev et al., *Comprehensive Composite Materials II* , (5), 130-157 (2018)
- 8) E. Volkmann et al., *Composites Part A*, **68**,19-28 (2015)
- 9) B. Jackson et al., “Oxide-Oxide Ceramic Matrix Composites–Enabling Widespread Industry Adoption” *3M technical paper*
- 10) C. J. Hull, *AFIT Scholar Student Graduate Works*, **3**,26 (2015)
- 11) Composite Materials Handbook-17-5A,79(2017)
- 12) S. C. B. Poway, et al., U. S. Pat. 20020197465(2002)
- 13) K. A. Keller et al., *Journal of the American Ceramic Society*, **86**(2), 325–32 (2003)
- 14) M. Schmücker, et al., *Materials Science and Engineering*, **557**,10-16 (2012)
- 15) D. Broek, *Elementary engineering fracture mechanism*, 3-23(1982)

